Nanospheres Delivering the EGFR TKI AG1478 Promote Optic Nerve Regeneration: The Role of Size for Intraocular Drug Delivery

Rebecca Robinson,[†] Stephen R. Viviano,[‡] Jason M. Criscione,[†] Cicely A. Williams,[§] Lin Jun,[⊥] James C. Tsai,[⊥] and Erin B. Lavik[∥,*]

[†]Department of Biomedical Engineering, Yale University, New Haven, Connecticut, United States, [‡]Yale Vision Core Facility, Yale University School of Medicine, New Haven, Connecticut, United States, [§]Interdepartmental Neuroscience Program, Yale University, New Haven, Connecticut, United States, [⊥]Department of Ophthalmology and Visual Science, Yale University School of Medicine, New Haven, Connecticut, United States, and [∥]Department of Biomedical Engineering, Case Western Reserve University, Cleveland, Ohio, United States

ABSTRACT Promoting nerve regeneration involves not only modulating the postinjury microenvironment but also ensuring survival of injured neurons. Sustained delivery of epidermal growth factor receptor (EGFR) tyrosine kinase inhibitors (TKIs) has been shown to promote the survival and regeneration of neurons, but systemic administration is associated with significant side effects. We fabricated poly(lactic-co-glycolic acid) (PLGA) microspheres and nanospheres containing the EGFR TKI 4-(3-chloroanilino)-6,7-dimethoxyquinazoline (AG1478) for intravitreal administration in a rat optic nerve crush injury model. Upon administration, less backflow from the injection site was observed when injecting nanospheres compared to microspheres. Two weeks after intravitreal delivery, we were able to detect microspheres and nanospheres in the vitreous using coumarin-6 fluorescence, but fewer microspheres were observed compared to the nanospheres. At four weeks only nanospheres could be detected. AG1478 microspheres and nanospheres promoted optic nerve regeneration at two weeks, and at four weeks evidence of regeneration was found only in the nanosphere-injected animals. This observation could be attributed to the ease of administration of the nanospheres *versus* the microspheres, which in turn led to an increased amount of spheres delivered to the vitreous in the nanosphere group compared to the microsphere group. These data provide evidence for use of PLGA nanospheres to deliver AG1478 intravitreally in a single administration to promote nerve regeneration.

KEYWORDS: optic nerve regeneration · nanospheres · microspheres · PLGA · epidermal growth factor receptor · AG1478

Epidermal growth factor receptor (EGFR) plays an important role in the developing and mature mammalian central nervous system (CNS). During embryonic and neonatal stages, EGFR is expressed in glia and neurons of mouse and rat brains.[1,2] In normal adult mice, rats, and humans EGFR is expressed in the ganglion cell and inner nuclear layers of the retina.[3] Certain EGFR ligands influence differentiation of neural progenitor cells (NPCs),[4] promote proliferation of NPCs and astrocytes,[5,6] promote survival of mature neurons *in vitro*,[5] and induce astrogliosis,[7] the process by which astrocytes change from a quiescent to a reactive, inhibitory phenotype. Mice lacking EGFR display postnatal neurodegeneration[8] and abnormal astrocyte development.[9]

Recent research has also examined the role of EGFR in CNS injury. The same EGFR ligands that promote proliferation and survival of neural cells may also contribute to the inhibitory nature of the scar environment postinjury. Transforming growth factor beta 1 (TGF-β1) and the EGFR ligand EGF greatly increase the production of several chondroitin sulfate proteoglycans (CSPGs), which are known to inhibit nerve regeneration following injury.[10] Two CSPGs, neurocan and phosphacan, are upregulated after CNS injury and astrogliosis and have been shown to inhibit growth of nerves following injury (for an excellent review see the work by Fawcett and Asher[11]). In addition, activation of EGFR causes astrocytes to change to a reactive phenotype that results in increased production of growth-inhibitory CSPGs.[12]

Strategies targeting inhibition of EGFR for nerve regeneration therapy include administration of reversible and irreversible small-molecule tyrosine kinase inhibitors (TKIs). For example, repeated administration of the EGFR TKI 4-(3-chloroanilino)-6,7-dimethoxyquinazoline (AG1478) (Figure S1), a reversible inhibitor, through drinking water in a chronic glaucoma model led to increased retinal ganglion cell survival for seven months,[12] and sustained delivery of the EGFR TKI 4-[(3-bromophenyl)amino]-6-acrylamidoquinazoline (PD168393), an irreversible inhibitor, or AG1478 in an optic nerve crush injury increased nerve regeneration over controls at

* Address correspondence to erin.lavik@case.edu.

Received for review November 19, 2010 and accepted May 28, 2011.

Published online May 28, 2011
10.1021/nn103146p

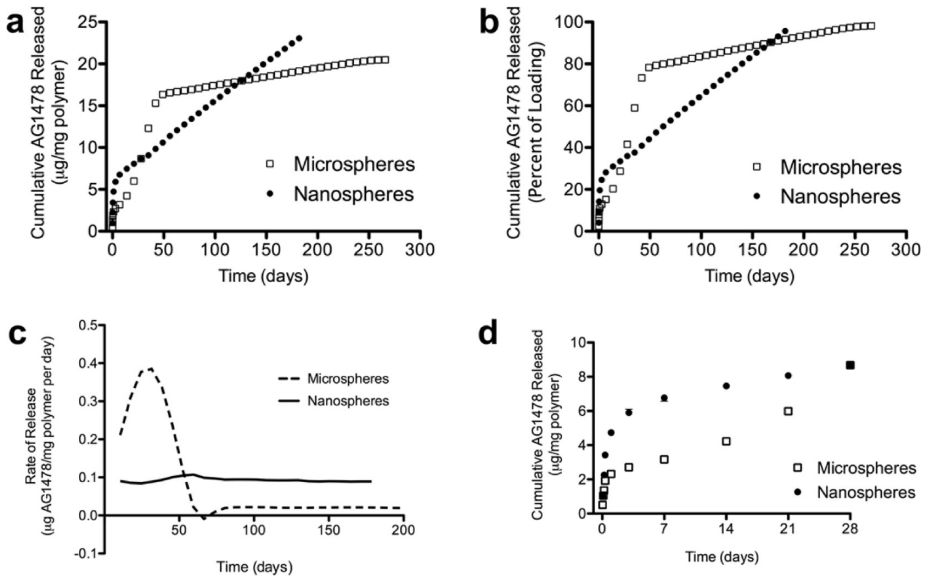

Figure 1. Characterization of AG1478 release from PLGA microspheres and nanospheres. (a) Cumulative release of AG1478 from PLGA microspheres (□) and nanospheres (●). (b) Cumulative release (percent of loading) of AG1478 from PLGA microspheres (□) and nanospheres (●). Data expressed as mean ± SD (n = 3). AG1478 was released over six months for both sphere types. (c) Rate of release of AG1478 after seven days from nanospheres (solid line) compared to microspheres (dashed line). After the initial burst, nanospheres release AG1478 at a constant rate, while microspheres release AG1478 fast, then slow. (d) Cumulative release of AG1478 up to 28 days from nanospheres (□) compared to microspheres (●). At 28 days both sphere sizes cumulatively release the same amount of AG1478. Data expressed as mean ± SD (n = 3).

two weeks.[13] While these drugs have been shown to promote neural protection and regeneration, the delivery of these drugs in these studies is not suitable for clinical therapy. Systemic administration of EGFR inhibitors is associated with dose-limiting side effects including skin rashes and diarrhea. Daily application of the drug to the optic nerve, as was done in the optic nerve crush model,[13] is not feasible. Sustained, local delivery is critical for these or similar drugs to be viable, and they must be administered in a manner that can be tolerated by patients.

We sought to develop a minimally invasive platform for sustained and controlled intraocular delivery of the EGFR TKI AG1478 that would promote optic nerve regeneration. Previously, we investigated formulation parameters for PLGA encapsulation of AG1478 in microspheres.[14] PLGA microspheres have been successfully delivered intravitreally in a number of animal models with no apparent side effects.[15,16] In the present study we developed PLGA nanospheres delivering AG1478 and compared the administration of microspheres and nanospheres to the vitreous of adult rat eyes after optic nerve crush injury and examined its effects on nerve regeneration at two weeks and four weeks. These time points were chosen from evidence in the literature that suggests that for significant and long-lasting functional recovery in the CNS to occur, neurons must be preserved, a permissive growth environment must be created, axonal elongation or regrowth must be promoted, and neuronal plasticity must be encouraged.[17] These issues need to be addressed both immediately after and for several weeks after injury. Regenerative fibers could be found in microsphere- and nanosphere-injected animals at two weeks, but at four weeks only nanosphere-injected animals maintained these fibers past the injury site. Our findings demonstrate that AG1478 spheres are a viable therapy to promote nerve regeneration. This platform of treatment has implications not only for acute CNS injury but for degenerative diseases (*e.g.*, glaucoma) as well.

RESULTS

Microsphere and Nanosphere Characterization. Encapsulation of AG1478 in nanospheres resulted in an increase in loading (23.3 ± 0.693 μg/mg polymer *vs* 21.8 ± 0.250 μg/mg polymer, mean ± SD) and encapsulation efficiency (79 ± 12% *vs* 67 ± 1.5%, mean ± SD) compared to microspheres. As previously reported, microspheres formulated as described can sustain release for over six months.[14] Nanospheres prepared in a similar manner also sustained release for over six months (182 days) (Figure 1a, b). However, unlike the microspheres, the release kinetics of the nanospheres did not follow a typical triphasic release for PLGA microspheres, with an initial burst, followed by a lag phase, and a secondary apparent-zero-order phase.[18] Instead, the nanospheres exhibited an initial burst followed by a zero-order phase (Figure 1c).[19]

Microspheres were fabricated with a volume-weighted mean diameter of 2.56 ± 1.90 μm as determined by the Coulter Multisizer, and nanospheres were fabricated with a mean diameter of 359 ± 54.0 nm, as determined by dynamic light scattering (DLS). Scanning electron microscopy (SEM) confirmed the diameters and revealed spheres that were heterogeneous in size with

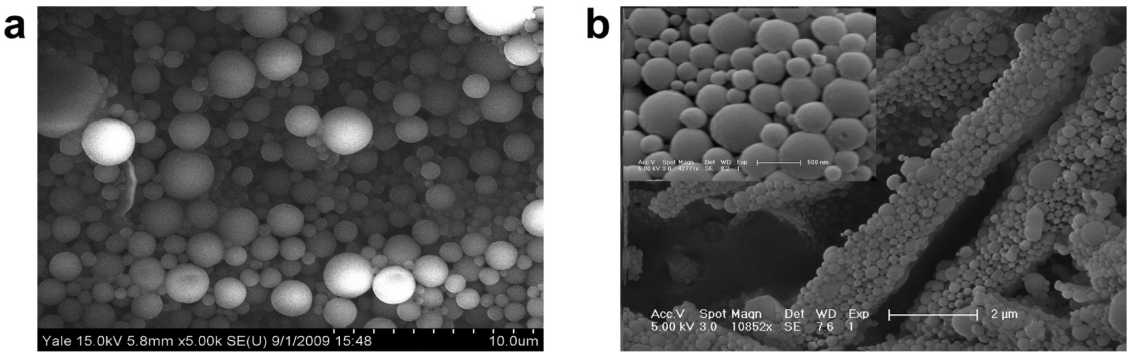

Figure 2. Morphology of AG1478 PLGA microspheres and nanospheres. (a) SEM micrograph of fabricated AG1478 microspheres. (b) Low-magnification SEM micrograph of fabricated AG1478 nanospheres. Inset is high magnification of low-magnification SEM.

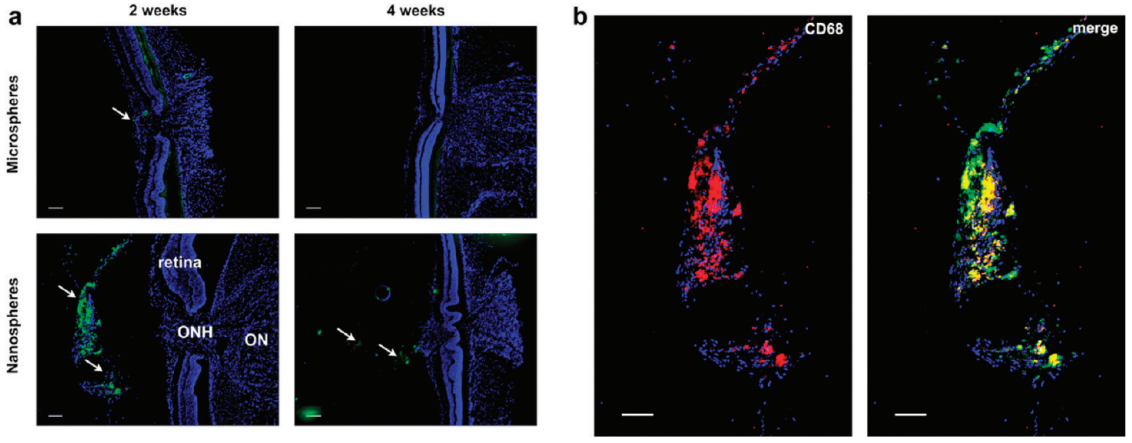

Figure 3. Distribution of coumarin-6 (C6) microspheres and nanospheres in the vitreous after intravitreal injection. (a) Immunofluorescence images of injected C6 (green) microspheres and nanospheres at two weeks and four weeks. Nuclei (blue) are labeled with DAPI. Arrows point to C6 microspheres and nanospheres. The weak green fluorescence observed adjacent to the retina but outside the vitreal space is a result of the autofluorescence of the retinal pigment epithelium and Bruch's membrane. (b) CD68 (red) immunostaining in the vitreous of the animal in the two-week nanosphere panel; cells surrounding the nanospheres are positive for CD68. Merge image of CD68 (red) and C6 (green) show co-localization of CD68 with nanospheres. ONH: optic nerve head, ON: optic nerve. Scale bars, 100 μm.

smooth surfaces. Figure 2a,b show AG1478 microspheres and nanospheres.

Distribution of Spheres after Injection. We encapsulated coumarin-6 (C6) in microspheres and nanospheres to track location and persistence of spheres after intravitreal injection.[20] Release of C6 from microspheres and nanospheres was less than 1.8% of loading at 14 days and less than 2.5% of loading at 28 days. Therefore, the presence of signal in the FITC excitation channel indicates spheres and not C6 alone over the time course studied here. From immunohistological analysis of the eye cups we were able to determine that injected microspheres and nanospheres locate to the vitreous after injection (Figure 3a); however at four weeks only nanospheres could be observed in the vitreous. Given the C6 fluorescence observed at two weeks in the microsphere group, we did not expect to find microspheres in the vitreous at four weeks.

To determine the source of the cells surrounding the C6 nanospheres at two weeks (Figure 3a), we stained for the rat macrophage and microglia marker CD68.[21] Immunofluorescence confirmed that some of the cells surrounding the C6 spheres were macrophages and/or microglia (Figure 3b). However, we observed very little CD68 immunostaining in the vitreous or retina of blank or AG1478 sphere-injected animals (Figure 4). Therefore, the macrophage/microglia response we observed in the C6 group was likely due to the C6, not the PLGA.

Axon Regeneration after AG1478 Sphere Injection. To first determine if intravitreal injection of AG1478 would be effective, we gave animals a one-time injection of a 10 μM concentration bolus of AG1478. This concentration was chosen on the basis of previous work by Korpivica *et al.*,[13] where AG1478 was delivered to the injured optic nerve via Gelfoam at a dose of 10 μM. Using an antibody against growth-associated protein 43 (GAP-43), we assessed the extent of axon regeneration in injured optic nerves. GAP-43-positive fibers could be observed past the crush site at two weeks, but not at four weeks (Figure 5).

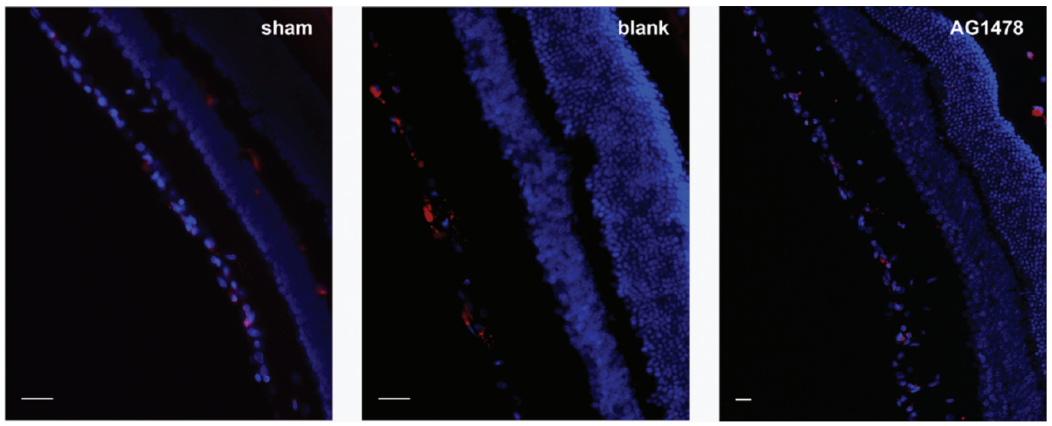

Figure 4. CD68 expression in the vitreous and retina of sham and sphere-injected animals. Representative images of CD68 (red) immunostaining in retinas from injured animals injected with blank or AG1478 spheres and animals that received no injection (sham). CD68 is expressed in the ganglion cell layer after optic nerve crush injury in all three groups, with no observed differences in immunostaining between the groups. No CD68-positive cells could be found in the vitreous of sham animals nor in sphere-injected animals. Nuclei (blue) are labeled with DAPI. Scale bars, 100 μm.

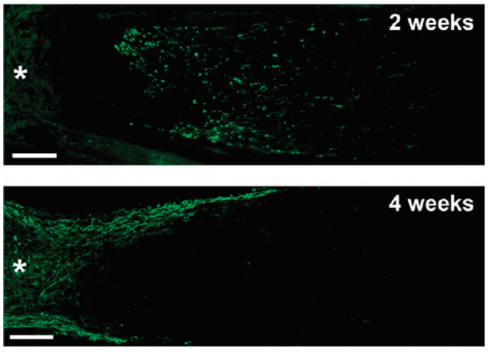

Figure 5. Confirming the feasibility of intravitreal delivery of AG1478. GAP-43 immunoreactivity (green) in the injured optic nerve of animals injected with a 10 μM concentration bolus of AG1478 to the vitreous at two weeks and four weeks. At two weeks, GAP-43-positive fibers can be observed past the injury site, but not through it. At four weeks, these fibers are no longer present. Asterisk indicates crush site. Scale bars, 100 μm.

After confirming the feasibility of delivering AG1478 to the vitreous, we assessed the extent of axon regeneration in injured optic nerves after a one-time intravitreal injection of either blank microspheres or nanospheres, or AG1478 microspheres or nanospheres. We administered spheres to injured animals and evaluated GAP-43 in the injured optic nerves. Rat vitreous volume is 56 μL,[22] and given our 5 μL injection of 50 mg/mL polymer spheres, the final intravitreal polymer concentration is 4.5 mg/mL. Using the *in vitro* controlled release curves the theoretical total amount of AG1478 delivered during the four-week period using this dose is 2.17 μg for microspheres and nanospheres, if the same amount of spheres was delivered for both the microsphere and nanosphere group. The dosage used for this study was determined and limited by the maximum amount of polymer that could be passed through a 30-gauge needle (*i.e.*, 50 mg/mL). Therefore, each group received the same amount of polymer and by four weeks the same amount of AG1478; however, the manner in which the drug was released differed depending on the size of the spheres (Figure 1d).

At two weeks, few differences were observed in GAP-43 immunostaining between groups (Figure 6a). However, the direction of fiber growth between the blank-sphere administered groups and the AG1478-sphere administered groups was noticeably different. In the animals that received blank spheres no fibers could be detected coming through the crush site, but in animals that received AG1478 spheres fibers could be observed originating form the crush site, suggesting growth of fibers through the injury site (Figure 6a). At four weeks, few if any fibers that were present at two weeks could be detected in the blank-sphere injected groups or in the AG1478 microsphere-injected group (Figure 7). However, GAP-43-positive fibers were present in the AG1478 nanosphere-injected group (Figures 6a and 7). Higher magnification imaging proximal to the crush site revealed several GAP-43-positive fibers originating from the site, suggesting growth of fibers through the injury site (Figure 6b). According to the graph in Figure 7, more fibers were present at 100 and 200 μm in the AG1478-nanosphere-injected group at four weeks (17.0 ± 3.61 and 10.7 ± 1.76 μm, respectively; $p < 0.001$; mean $\pm$ SEM) compared to the AG1478-microsphere-injected group (2.00 ± 0.58 and 0.33 ± 0.33 μm, respectively; $p < 0.001$; mean $\pm$ SEM). In addition, as indicated by the arrows in Figure 6b, in some cases fibers extended up to 300 μm past the injury site.

Recovery of AG1478 from Vitreous after Sphere Injection. In addition to examining GAP-43 immunostaining, we measured AG1478 from the vitreous of injured animals after injection. Preclinical studies using mice have indicated that the plasma elimination half-life of AG1478 after bolus intravenous administration is 30–48 min.[23] To determine vitreous drug concentration after injection, AG1478 was extracted from the vitreous of AG1478-sphere-injected rats and quantified

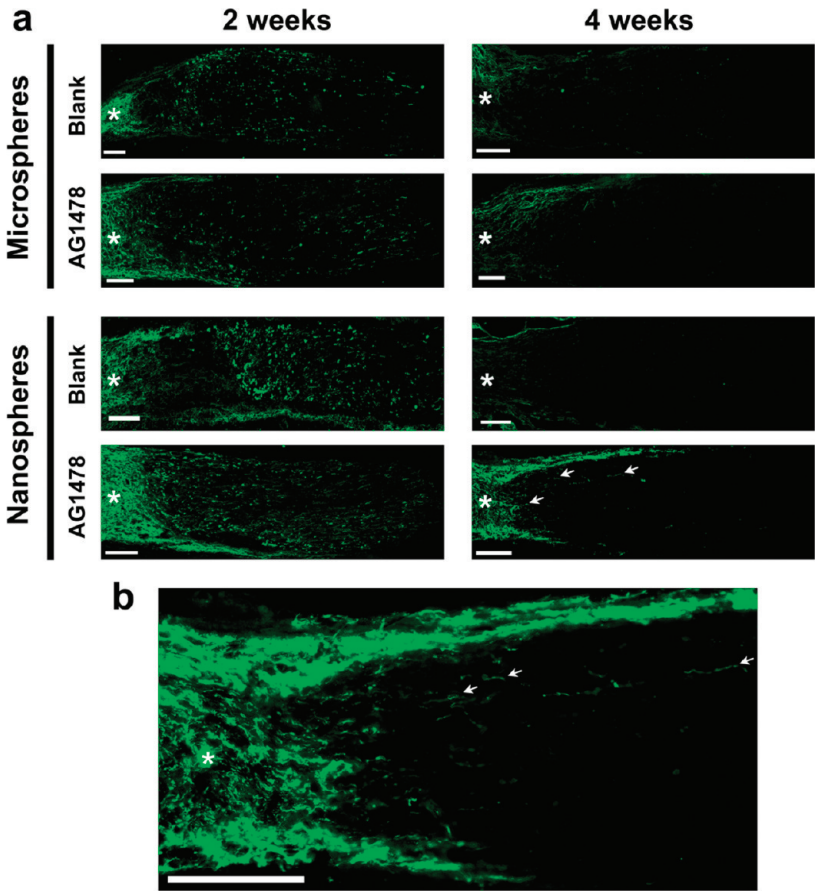

Figure 6. GAP-43 expression in the injured optic nerve after intravitreal injection of AG1478 microspheres and nanospheres. (a) GAP-43 immunostaining (green) in injured optic nerves at two weeks and four weeks after injection of blank and AG1478 microspheres or nanospheres. Fibers in the blank-sphere-injected groups do not originate from the injury site; instead they appear to originate from transected axons distal to the injury site. Numerous fibers originating from the injury site can be observed in the AG1478-sphere-injected groups. At four weeks, no fibers were observed in the blank-sphere-injected groups or the AG1478-microsphere-injected group. Arrows point to fibers that can be observed in the AG1478-nanosphere-injected group. (b) Higher magnification of the area proximal to the injury site in the four-week AG1478 nanosphere panel confirms that the fibers are originating from the injury site, and arrows show fibers extending 100−200 μm past the injury site. Asterisk indicates crush site. Scale bars, 100 μm.

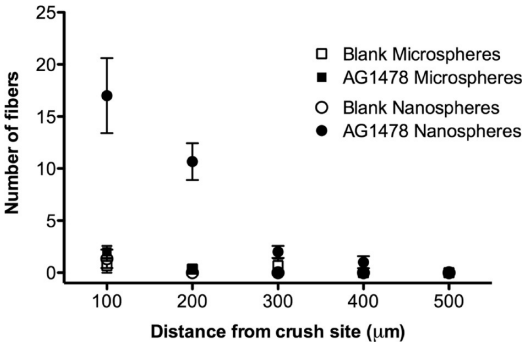

Figure 7. Quantification of GAP-43 fibers at 4 weeks. Average number of fibers present in each group at 100, 200, 300, 400, and 500 μm past the crush site. There is a significant ($p < 0.001$) difference in the number of fibers present 100 and 200 μm past the crush site in the AG1478-nanosphere-injected group compared to the other groups. Data expressed as mean ± SEM ($n = 3$).

using high-performance liquid chromatography (HPLC); as a control, vitreous from blank-sphere-injected and non-injured rats was also quantified using HPLC. No AG1478 could be detected at two weeks in animals injected with AG1478 microspheres or blank microspheres; however, AG1478 was detected (2.14 ± 1.62 μg/mL, $n = 3$; 6.41 ± 4.85% of injected dose; mean ± SD) at two weeks in nanosphere-injected animals. At four weeks no AG1478 could be detected in either group or control animals. The manner in which the vitreous is collected from enucleated eyes results in some loss of vitreous and therefore some loss of AG1478, thus resulting in an inability to recover all AG1478 from the vitreous. At four weeks, very little C6 fluorescence was observed in the nanosphere group; therefore, fewer spheres present combined with the collection protocol for vitreous could explain the lack of AG1478 detected at four weeks.

Glial Scar Changes after AG1478 Sphere Injection. Given the positive results for GAP-43 fibers, we investigated if these observed effects are due to the mechanisms currently described in the literature. AG1478 is implicated in modulating the postinjury environment through diminishing production of CSPGs in the glial scar.[10,13] Therefore, we examined immunostaining of glial fibrillary acidic protein (GFAP) for astrocytes, and

the expression of neurocan and phosphacan, CSPGs that have been shown to inhibit axon growth after injury.[11] Figure S2a shows representative images of GFAP, neurocan, and phosphacan immunostaining at two and four weeks. At two weeks, no difference in GFAP immunostaining was observed between groups (Figure S2b); however at four weeks significant differences were observed between all sphere-injected groups. In particular, AG1478 nanosphere-injected animals had significantly higher GFAP immunostaining compared to AG1478 microsphere-injected (p = 0.0491) and blank-nanosphere-injected (p = 0.0026) animals. While neurocan, absent in uninjured mature optic nerves, was upregulated after injury, no differences in neurocan immunostaining were observed between the groups at either time point (Figure S2c). In addition, no significant differences in phosphacan immunostaining were observed between the groups at either time point (Figure S2d). However, a trend toward lower phosphacan immunostaining across all groups at four weeks was observed.

DISCUSSION AND CONCLUSIONS

When developing a therapy, it is important to have a means of administration that is not only safe and effective but also delivered in a manner that is amenable to the patient. TKIs have shown promise for neural regeneration, but local delivery to the optic nerve is a challenging approach. Intravitreal administration is well tolerated by patients, but intravitreal bolus injection of TKIs is not effective to produce regeneration. The drug requires a vehicle that permits simple administration and sustained delivery. As we see in this work, formulation is not the only factor in determining long-term delivery; size has a great impact on the residence of the spheres and ultimately on regeneration.

This work demonstrates the successful encapsulation and fabrication of AG1478 microspheres and nanospheres for intravitreal delivery to enhance optic nerve regeneration. We show localization of injected spheres to the vitreous after injection and show persistence of injected nanospheres out to four weeks. In addition, this study demonstrates the feasibility of intravitreal delivery of AG1478 in bolus form and in a controlled-release platform. Our results provide the first evidence that AG1478 can be effective in promoting optic nerve regeneration for up to four weeks when delivered intravitreally using degradable PLGA nanospheres.

Our previous work examined encapsulation of AG1478 in PLGA microspheres. In this study we wanted to decrease the size of the spheres to facilitate intravitreal injection of the spheres through a 30-gauge needle. When comparing the two release profiles, we expected the profile for the nanospheres to be similar to the profile for the microspheres except with a larger burst, which is typical for nanospheres.[24−26] After the larger initial burst, the nanospheres displayed a linear release profile (Figure 1a) and slower release kinetics (Figure 1c) compared to the microspheres. The differences observed in the release rates could be due to the internal structure of the network of the polymer and drug. Given the characteristics of the release profiles—longer than expected release and in the case of the nanospheres linear release—it is apparent that there have been changes to the polymer−drug interaction, the crystallinity of the polymer, and/or the density of the overall sphere structure, can affect the release kinetics.[27,28] Microspheres could have a less rigid structure, thereby allowing for greater access of water to the interior structure of the sphere resulting in faster release, and *vice versa* for nanospheres.[29,30]

Encapsulation of C6 in microspheres and nanospheres provided not only a useful tool for evaluating the location and persistence of spheres after intravitreal injection but also a qualitative measure of the amount of polymer that is successfully injected. From immunohistological analysis of the eye cups we were able to determine that injected microspheres and nanospheres locate to the vitreous after injection, however to a lesser degree in the case of microspheres. At two weeks, we observed less C6 fluorescence in the vitreous, qualitatively, in the microsphere group. This difference could be attributed to the higher amount of backflow experienced during injection of microspheres compared to nanospheres. Alternatively, this difference could be attributed to the significant differences in sphere size. Smaller spheres, such as the nanospheres, would have a higher number of spheres per unit volume compared to larger spheres, such as microspheres. Consequently, the decrease in C6 immunofluorescence in the microsphere-injected animals could be due to fewer spheres injected per given 5 μL volume compared to the nanosphere-injected animals.

The decrease in number of spheres in the microsphere-injected animals *versus* the nanosphere-injected animals could also explain the differences observed in the GAP-43 immunostaining between microsphere- and nanosphere-injected animals. At two weeks more fibers are observed proximal to the crush site and through the crush site in the AG1478 nanosphere group *versus* the AG1478 microsphere group (Figure 6a). At four weeks, GAP-43-positive fibers that were present in the AG1478 microsphere group were absent and GAP-43 immunostaining at the crush site had significantly diminished, compared to the AG1478 nanosphere group (Figures 6a and 7). These differences could be attributed to fewer spheres present in the microsphere group compared to the nanosphere group, thereby leading to less AG1478 administered in the microsphere group.

Immunohistochemical staining of the optic nerves for GFAP showed a higher amount of GFAP staining in the AG1478 nanosphere group compared to the AG1478 microsphere group. This increase in GFAP staining may initially seem counterintuitive; however, closer examination of the images (Figure S2b) reveals a greater degree of orientation of the GFAP-positive cells as compared to the two-week images. Therefore at four weeks, the astrocytes could be arranging in a more organized fashion that resembles uninjured tissue and indicates possible recovery from the initial injury.

Other groups have reported extensively on the role AG1478 plays in modulating the postinjury environment, specifically its role in diminishing production of CSPGs in the glial scar.[10,13] Although we observed no significant decreases in the CSPGs neurocan and phosphacan in the injured optic nerves after AG1478 sphere administration, GAP-43-positive fibers are present past the injury site out to four weeks. There have been reports in the literature of off-target neuroprotective effects of AG1478.[31,32] Specifically, studies suggest that AG1478 may also act independently of EGFR and affects other signaling pathways in the cells. Therefore, the regenerative effects we see could be due to these off-target effects. However, further immunohistochemical and immunoblot analyses would need to be done to confirm these hypotheses.

These studies provide evidence for use of this platform to promote regeneration in acute CNS injury and demonstrate the advantages of our system *versus* current means of administration, namely, that it is minimally invasive and capable of delivering relevant doses of AG1478 over sustained periods. Our results provide the first evidence that AG1478 can be effective in promoting optic nerve regeneration over extended periods when delivered intravitreally using degradable PLGA nanospheres. Furthermore, this system can be modified to deliver more AG1478 by either increasing the amount of the co-solvent present or increasing the loading. In conclusion, this work provides evidence for the preference of nanospheres over microspheres for sustained ophthalmic drug delivery. We believe this work demonstrates the promise of sustained delivery of EGFR TKIs using PLGA nanospheres as a therapy for optic nerve regeneration and other CNS injuries.

METHODS

Fabrication of AG1478 and C6 Microspheres and Nanospheres. Microspheres were prepared using an oil-in-water with co-solvent single emulsion solvent evaporation technique, as previously described.[14] Briefly, 5 mg of AG1478 or 10 mg of coumarin-6 dissolved in dimethyl sulfoxide (DMSO) was added to 200 mg of PLGA 503H in a 2.5 mL mixture of dichloromethane (DCM) solvent and trifluoroethanol (TFE) co-solvent (1:5 DCM/TFE, v/v). The resulting PLGA-AG1478 or PLGA-C6 solution was added dropwise to 4 mL of 5% PVA while vortexing. This emulsion was added dropwise to 100 mL of 5% PVA and stirred for 3 h. The microspheres were centrifuged at 12 000 rpm for 15 min, washed with deionized water for three cycles, flash frozen, lyophilized, and stored at −20 °C.

Nanospheres were also fabricated using an oil-in-water with co-solvent single emulsion solvent evaporation technique, however, with the addition of sonication at 38% power for 30 s. After sonication, the emulsion was added dropwise to 100 mL of 5% PVA and stirred for 3 h at room temperature. Nanospheres were washed and stored as described above.

Blank microspheres and nanospheres were made under identical conditions for each preparation, except no AG1478 or C6 was added.

Determination of AG1478 Sphere Loading. To determine loading of AG1478 microspheres and nanospheres, 5 mg of AG1478 spheres or blank spheres was placed in 1.5 mL tubes. One milliliter of DMSO was added to the tubes and vortexed to completely dissolve the spheres.[33] The concentration of AG1478 in the spheres was determined using a SpectraMax M5 ultraviolet (UV) spectrophotometer (Molecular Devices; Sunnyvale, CA) at 330 nm.[34] Encapsulation efficiency was determined by dividing the actual amount of drug loaded into the spheres by the amount of drug added to the emulsion preparation (5 mg).

Determination of AG1478 Released from Spheres. A stock solution of InSolution AG1478 (EMD Biosciences; Gibbstown, NJ) at 10 mM concentration was diluted in PBS and used to produce a standard curve that showed linearity and reproducibility over the concentration range 0.39−100 μM (0.12−31.6 μg/mL) ($r^2 >$ 0.999). In 1.5 mL tubes, 10 mg of AG1478 spheres or blank spheres was reconstituted in 1 mL of PBS. Samples were prepared in triplicate. Mixtures were then incubated at 37 °C on a rotating shaker (Barnstead/Thermolyne; Dubuque, IA). At specific time points—1, 5, and 8 h and 1, 3, 5, and 7 days and once every 7 days afterward until no AG1478 could be measured—the mixture was centrifuged at 13 000 rpm for 20 min and the supernatant collected. One milliliter of PBS was added to the tubes to replace the supernatant, and the mixture was then vortexed to resuspend the spheres. The tubes were returned to the shaker until the next time point. Collected supernatants were stored at −20 °C until they could be analyzed using UV spectroscopy at 330 nm.

Determination of C6 Sphere Loading. To determine loading of C6 micro- and nanospheres, 5 mg of C6 microspheres or blank microspheres was placed in 1.5 mL tubes. One milliliter of DMSO was added to the tubes and vortexed to completely dissolve the microspheres. The concentration of C6 in the spheres was determined using a SpectraMax M5 fluorescence microplate reader at 444/538 nm (Ex/Em). Encapsulation efficiency was determined by dividing the actual amount of C6 loaded into the microspheres by the amount of C6 added to the emulsion preparation (10 mg).

Determination of C6 Released from Spheres. In 1.5 mL tubes, 5 mg of C6 or blank microspheres or nanospheres was reconstituted in 1 mL of phosphate-buffered saline (PBS, pH 7.4). Samples were prepared in triplicate. Mixtures were then incubated at 37 °C on a rotating shaker. At specific time points—1, 5, and 8 h and 1, 3, 5, and 7 days and once every 7 days afterward—the mixture was centrifuged at 13 000 rpm for 20 min and the supernatant collected. One milliliter of PBS was added to the tubes to replace the supernatant, and the mixture was then vortexed to resuspend the spheres. The tubes were returned to the shaker until the next time point. Collected supernatants were freeze-dried, reconstituted in 1.0 mL of DMSO, and then analyzed at 444/538 nm (Ex/Em) for C6 content.

Evaluation of C6 and AG1478 Microspheres and Nanospheres *in Vivo*. Sprague−Dawley female rats, 6−8 weeks in age (180−200 g), were purchased from Charles River Laboratories (Wilmington, MA) and maintained in temperature-controlled rooms on a 12 h light/dark cycle. Experiments were performed in accordance

with procedures approved by Animal Care and Use Committees of Yale University and follow the National Institutes of Health Guide for the Care and Use of Laboratory Animals and the Association for Research in Vision and Ophthalmology Statement for the Use of Animals in Ophthalmology and Visual Research. Animals were sacrificed and eyes were enucleated two weeks and four weeks after injury. Further details of the surgical care of the animals are included in the Supporting Information.

Optic Nerve Crush Injury. The optic nerve was crushed unilaterally for each experimental group. The nerve was exposed and isolated by a transverse incision carried through the skin 3 mm from the corner of the eye. Using iris scissors a small hole was cut in the exposed tissue and fascia along the border of the globe of the eye. Forceps were used to bluntly dissect between the globe and the orbit until the optic nerve at the back of globe was visualized. The optic nerve was crushed for 10 s with forceps. No loss of retinal circulation was confirmed by ophthalmoscopic observation.

Intravitreal Injection of AG1478 and Spheres. Five to 10 minutes after the crush injury, animals were injected intravitreally with a 50 mg polymer/mL concentration of C6 microspheres ($n = 9$), C6 nanospheres ($n = 8$), AG1478 microspheres ($n = 12$), AG1478 nanospheres ($n = 12$), blank microspheres ($n = 9$), or blank nanospheres ($n = 6$) suspended in 1× PBS, or a 10 μM concentration of AG1478 in 1× PBS ($n = 12$). A single dose of bolus AG1478 or AG1478 micro- or nanospheres in a volume of 5 μL was injected into the vitreous under a dissecting microscope using a 25 μL Hamilton gastight syringe (Hamilton Co.; Reno, NV) with a 30-gauge needle. A 27-gauge needle was first used to make a punch incision 0.5 mm posterior to the temporal limbus, and the needle was then inserted through the incision, approximately 1.5 mm deep, angled toward the optic nerve until the tip of the needle was seen in the center of the vitreous. Intravitreal delivery of spheres was confirmed by observing a white or yellow suspension in the posterior vitreous under the microscope. Lens injury has been shown to increase regeneration and RGC survival;[35,36] therefore eyes with lens injury from injection were excluded from the study. Lens injury was confirmed by examining each treatment eye for cataract prior to tissue processing.

Immunohistochemistry. Eyes were enucleated and fixed in 4% paraformaldehyde, and the optic nerves were dissected free of surrounding tissues. Fixed tissues were washed in PBS, soaked in 30% sucrose overnight, embedded in OCT (Sakura Finetechnical; Tokyo, Japan), and cryo-sectioned to 14 μm thick longitudinal sections of optic nerve and 14 μm thick cross sections of eye cups.

Optic nerve and eye cup tissue was blocked and stained with antibodies to proteins of interest. Optic nerves and eye cups from noninjured animals were used as negative controls for GAP-43 and CD68 immunostaining. For detailed information on the antibodies used, please see the Supporting Information.

For GAP-43 staining of the optic nerve, 12−16 sections from all animals in each group were stained and imaged with a Zeiss AxioCam MRm camera mounted on a Zeiss Axiovert 200 M inverted microscope using a 10× objective (N.A. 0.50; Zeiss) or a 20× objective (N.A. 0.75; Zeiss). Images were analyzed with Zeiss AxioVision 4.7 software and Adobe Photoshop CS5 Extended software (Adobe Systems, Inc.; San Jose, CA). GAP-43-positive fibers caudal to the crush site were imaged and examined. The crush site was identified by (1) a concentrated cluster of disorganized DAPI-positive nuclei and (2) intense and concentrated GAP-43 immunostaining. For GAP-43 quantification at four weeks, fibers were counted by eye up to 500 μm from the crush site at 100 μm increments using the count and ruler tools in Adobe Photoshop CS5 Extended (Adobe Systems, Inc.; San Jose, CA). All images were taken at the same exposure for each time point and group. The offset and gain of the camera were held constant between different images.

For GFAP, CD68, neurocan, and phosphacan staining of the optic nerve, three animals from each group were chosen randomly and analyzed. Three images total were taken per nerve: one caudal to the crush site, one at the crush site, and one rostral to the crush site. For each stain, all images were taken at the same exposure for each time point and group. Images for GFAP and CD68 were acquired using a 10× objective (N.A. 0.50; Zeiss). Images for neurocan and phosphacan were acquired using a 20× objective (N.A. 0.75; Zeiss). Area of fluorescence per high-powered field was quantified by thresholding the lower limit of each image and measuring area using ImageJ software (NIH; Bethesda, MD). Lower limit was held constant for each treatment group.

Eye cups from C6-injected animals were stained for CD68 and imaged to locate spheres after injection. Images were acquired using a 5× objective (N.A. 0.25; Zeiss).

A two-way ANOVA was used to determine differences among groups and time points when evaluating the GAP-43, GFAP, neurocan, and phosphacan immunostaining, with a Bonferroni post-test to evaluate significance. A p value of <0.05 was considered statistically significant.

Acknowledgment. This work was funded by a United States National Institutes of Health National Research Service Award from the National Eye Institute (F31EY019441; R.R.), a United States National Institutes of Health Neuroengineering training grant (T90DK070068; R.R.), a United States National Institutes of Health Medical Scientist Training Program training grant (T32GM07025; C. A.W.), a United States National Institutes of Health Director's New Innovator Award Program grant (DP2OD007338; E.B.L.), The Glaucoma Foundation (Research Grant, E.B.L. and R.R.), and Research to Prevent Blindness (Departmental Challenge Grant, J.C.T.). Other funding was provided by the generous support of R. and G. Siegal and a generous gift of C. Sirot. The authors thank Professor A. Levitzki (Hebrew University of Jerusalem; Jerusalem, Israel) for contribution of the internal standard AG1557, and Dr. E. Steenblock for assistance with the Table of Contents graphic.

Supporting Information Available: Diagram of the chemical structure of AG1478 (Figure S1), schematic of the surgical approach (Figure S2), glial scar analysis (Figure S3), and detailed experimental methods. This material is available free of charge *via* the Internet at http://pubs.acs.org.

REFERENCES AND NOTES

1. Adamson, E. D.; Meek, J. The Ontogeny of Epidermal Growth Factor Receptors During Mouse Development. *Dev. Biol.* **1984**, *103*, 62–70.
2. Kornblum, H.; Hussain, R.; Bronstein, J.; Gall, C.; Lee, D.; Seroogy, K. Prenatal Ontogeny of the Epidermal Growth Factor Receptor and Its Ligand, Transforming Growth Factor Alpha, in the Rat Brain. *J. Comp. Neurol.* **1997**, *380*, 243–261.
3. Chen, H.; Liu, B.; Neufeld, A. H. Epidermal Growth Factor Receptor in Adult Retinal Neurons of Rat, Mouse, and Human. *J. Comp. Neurol.* **2007**, *500*, 299–310.
4. Reynolds, B.; Tetzlaff, W.; Weiss, S. A Multipotent EGF-Responsive Striatal Embryonic Progenitor Cell Produces Neurons and Astrocytes. *J. Neurosci.* **1992**, *12*, 4565–4574.
5. Kornblum, H.; Zurcher, S.; Werb, Z.; Derynck, R.; Seroogy, K. Multiple Trophic Actions of Heparin-Binding Epidermal Growth Factor (HB-EGF) in the Central Nervous System. *Eur. J. Neurosci.* **1999**, *11*, 3236–3246.
6. Levison, S.; Jiang, F.; Stoltzfus, O.; Ducceschi, M. Il-6-Type Cytokines Enhance Epidermal Growth Factor-Stimulated Astrocyte Proliferation. *Glia* **2000**, *32*, 328–337.
7. Rabchevsky, A.; Weinitz, J.; Coulpier, M.; Fages, C.; Tinel, M.; Junier, M. A Role for Transforming Growth Factor Alpha as an Inducer of Astrogliosis. *J. Neurosci.* **1998**, *18*, 10541–10552.
8. Sibilia, M.; Steinbach, J. P.; Stingl, L.; Aguzzi, A.; Wagner, E. F. A Strain-Independent Postnatal Neurodegeneration in Mice Lacking the EGF Receptor. *Embo J.* **1998**, *17*, 719–31.
9. Kornblum, H.; Hussain, R.; Wiesen, J.; Miettinen, P.; Zurcher, S.; Chow, K.; Derynck, R.; Werb, Z. Abnormal Astrocyte Development and Neuronal Death in Mice Lacking the Epidermal Growth Factor Receptor. *J. Neurosci. Res.* **1998**, *53*, 697–717.
10. Smith, G.; Strunz, C. Growth Factor and Cytokine Regulation of Chondroitin Sulfate Proteoglycans by Astrocytes. *Glia* **2005**, *52*, 209–218.

11. Fawcett, J.; Asher, R. The Glial Scar and Central Nervous System Repair. *Brain Res. Bull.* **1999**, *49*, 377–391.
12. Liu, B.; Chen, H.; Johns, T.; Neufeld, A. Epidermal Growth Factor Receptor Activation: An Upstream Signal for Transition of Quiescent Astrocytes into Reactive Astrocytes after Neural Injury. *J. Neurosci.* **2006**, *26*, 7532–7540.
13. Koprivica, V.; Cho, K.; Park, J.; Yiu, G.; Atwal, J.; Gore, B.; Kim, J.; Lin, E.; Tessier-Lavigne, M.; Chen, D.; *et al*. EGFR Activation Mediates Inhibition of Axon Regeneration by Myelin and Chondroitin Sulfate Proteoglycans. *Science* **2005**, *310*, 106–110.
14. Robinson, R.; Bertram, J. P.; Reiter, J. L.; Lavik, E. B. New Platform for Controlled and Sustained Delivery of the EGF Receptor Tyrosine Kinase Inhibitor AG1478 Using Poly-(lactic-co-glycolic Acid) Microspheres. *J Microencapsul.* **2010**, *27*, 263–271.
15. Duvvuri, S.; Janoria, K.; Pal, D.; Mitra, A. Controlled Delivery of Ganciclovir to the Retina with Drug-Loaded Poly(D,L-Lactide-Co-Glycolide) (PLGA) Microspheres Dispersed in PLGA-PEG-PLGA Gel: A Novel Intravitreal Delivery System for the Treatment of Cytomegalovirus Retinitis. *J. Ocul. Pharmacol. Ther.* **2007**, *23*, 264–274.
16. Ward, M. S.; Khoobehi, A.; Lavik, E. B.; Langer, R.; Young, M. J. Neuroprotection of Retinal Ganglion Cells in DBA/2J Mice with GDNF-Loaded Biodegradable Microspheres. *J. Pharm. Sci.* **2007**, *96*, 558–568.
17. Ellis-Behnke, R. Nano Neurology and the Four P's of Central Nervous System Regeneration: Preserve, Permit, Promote, Plasticity. *Med. Clin. North Am.* **2007**, *91*, 937–962.
18. Zolnik, B. S.; Burgess, D. J. Effect of Acidic pH on PLGA Microsphere Degradation and Release. *J. Controlled Release* **2007**, *122*, 338–344.
19. Jeon, O.; Kang, S.-W.; Lim, H.-W.; Hyung Chung, J.; Kim, B.-S. Long-Term and Zero-Order Release of Basic Fibroblast Growth Factor from Heparin-Conjugated Poly(L-Lactide-Co-Glycolide) Nanospheres and Fibrin Gel. *Biomaterials* **2006**, *27*, 1598–1607.
20. Eley, J. G.; Pujari, V. D.; Mclane, J. Poly (Lactide-Co-Glycolide) Nanoparticles Containing Coumarin-6 for Suppository Delivery: In Vitro Release Profile and in Vivo Tissue Distribution. *Drug Delivery* **2004**, *11*, 255–261.
21. White, R.; Yin, F.; Jakeman, L. TGF-[Alpha] Increases Astrocyte Invasion and Promotes Axonal Growth into the Lesion Following Spinal Cord Injury in Mice. *Exp. Neurol.* **2008**, *214*, 10–24.
22. Berkowitz, B. A.; Lukaszew, R. A.; Mullins, C. M.; Penn, J. S. Impaired Hyaloidal Circulation Function and Uncoordinated Ocular Growth Patterns in Experimental Retinopathy of Prematurity. *Invest. Ophthalmol. Vis. Sci.* **1998**, *39*, 391–396.
23. Ellis, A.; Doherty, M.; Walker, F.; Weinstock, J.; Nerrie, M.; Vitali, A.; Murphy, R.; Johns, T.; Scott, A.; Levitzki, A.; *et al*. Preclinical Analysis of the Analinoquinazoline AG1478, a Specific Small Molecule Inhibitor of Egf Receptor Tyrosine Kinase. *Biochem. Pharmacol.* **2006**, *71*, 1422–1434.
24. Dawes, G. J. S.; Fratila-Apachitei, L. E.; Mulia, K.; Apachitei, I.; Witkamp, G.-J.; Duszczyk, J. Size Effect of PLGA Spheres on Drug Loading Efficiency and Release Profiles. *J. Mater. Sci. Mater. Med.* **2009**, *20*, 1089–1094.
25. Chorny, M.; Fishbein, I.; Danenberg, H. D.; Golomb, G. Lipophilic Drug Loaded Nanospheres Prepared by Nanoprecipitation: Effect of Formulation Variables on Size, Drug Recovery and Release Kinetics. *J. Controlled Release* **2002**, *83*, 389–400.
26. Mainardes, R. M.; Evangelista, R. C. Praziquantel-Loaded PLGA Nanoparticles: Preparation and Characterization. *J. Microencapsul.* **2005**, *22*, 13–24.
27. Alexis, F. Factors Affecting the Degradation and Drug-Release Mechanism of Poly(lactic acid) and Poly[(lactic acid)-co-(glycolic acid)]. *Polym. Int.* **2005**, *54*, 36–46.
28. Shive, M.; Anderson, J. Biodegradation and Biocompatibility of PLA and PLGA Microspheres. *Adv. Drug Delivery Rev.* **1997**, *28*, 5–24.
29. Chorny, M.; Fishbein, I.; Danenberg, H. D.; Golomb, G. Study of the Drug Release Mechanism from Tyrphostin AG-1295-Loaded Nanospheres by in Situ and External Sink Methods. *J. Controlled Release* **2002**, *83*, 401–114.
30. Fu, K.; Pack, D. W.; Klibanov, A. M.; Langer, R. Visual Evidence of Acidic Environment within Degrading Poly-(Lactic-Co-Glycolic Acid) (PLGA) Microspheres. *Pharm. Res.* **2000**, *17*, 100–106.
31. Ahmed, Z.; Jacques, S. J.; Berry, M.; Logan, A. Epidermal Growth Factor Receptor Inhibitors Promote CNS Axon Growth through Off-Target Effects on Glia. *Neurobiol. Dis.* **2009**, *36*, 142–50.
32. Douglas, M. R.; Morrison, K. C.; Jacques, S. J.; Leadbeater, W. E.; Gonzalez, A. M.; Berry, M.; Logan, A.; Ahmed, Z. Off-Target Effects of Epidermal Growth Factor Receptor Antagonists Mediate Retinal Ganglion Cell Disinhibited Axon Growth. *Brain* **2009**, *132*, 3102–3121.
33. Gupta, R. K.; Chang, A. C.; Griffin, P.; Rivera, R.; Guo, Y. Y.; Siber, G. R. Determination of Protein Loading in Biodegradable Polymer Microspheres Containing Tetanus Toxoid. *Vaccine* **1997**, *15*, 672–678.
34. Ellis, A.; Nice, E.; Weinstock, J.; Levitzki, A.; Burgess, A.; Webster, L. High-Performance Liquid Chromatographic Analysis of the Tyrphostin AG1478, a Specific Inhibitor of the Epidermal Growth Factor Receptor Tyrosine Kinase, in Mouse Plasma. *J. Chromatogr. B: Biomed. Sci. Appl.* **2001**, *754*, 193–199.
35. Fischer, D.; Heiduschka, P. Thanos, Lens-Injury-Stimulated Axonal Regeneration Throughout the Optic Pathway of Adult Rats. *Exp. Neurol.* **2001**, *172*, 257–272.
36. Leon, S.; Yin, Y.; Nguyen, J.; Irwin, N.; Benowitz, L. Lens Injury Stimulates Axon Regeneration in the Mature Rat Optic Nerve. *J. Neurosci.* **2000**, *20*, 4615–4626.